

**$D\bar{D}$  Correlations in Photoproduction**

M.P.Alvarez<sup>1</sup>, R.Barate<sup>2a</sup>, D.Bloch<sup>3</sup>, P.Bonamy<sup>4</sup>, P.Borgeaud<sup>4</sup>, M.Burchell<sup>5</sup>,  
 H.Burmeister<sup>2</sup>, J.M.Brunet<sup>6</sup>, F.Calvino<sup>1b</sup>, M.Cattaneo<sup>5</sup>, J.M.Crespo<sup>1</sup>,  
 B.D'Almagne<sup>7</sup>, M.David<sup>4</sup>, L.Di Ciaccio<sup>2c</sup>, J.Dixon<sup>5</sup>, P.Druet<sup>7</sup>, A.Duane<sup>5</sup>,  
 J.P.Engel<sup>3</sup>, A.Ferrer<sup>2d</sup>, T.A.Filipas<sup>8</sup>, E.Fokitis<sup>8</sup>, R.W.Forty<sup>5</sup>, P.Foucault<sup>3</sup>,  
 E.N.Gazis<sup>8</sup>, J.P.Gerber<sup>3</sup>, Y.Giomataris<sup>2</sup>, T.Hofmohl<sup>9</sup>, E.C.Katsoufis<sup>8</sup>,  
 M.Koratzinos<sup>2,5,7</sup>, C.Krafft<sup>7</sup>, B.Lefievre<sup>6</sup>, Y.Lemoigne<sup>4</sup>, A.Lopez<sup>2,7e</sup>,  
 W.K.Lui<sup>10</sup>, C.Magneville<sup>4</sup>, A.Maltezos<sup>8</sup>, J.G.McEwen<sup>10</sup>, T.Papadopoulou<sup>8</sup>,  
 B.Pattison<sup>2</sup>, D.Poutot<sup>6</sup>, M.Primout<sup>4</sup>, H.Rahmani<sup>8</sup>, P.Roudeau<sup>7</sup>, C.Seez<sup>5</sup>,  
 J.Six<sup>7</sup>, R.Strub<sup>3</sup>, D.Treille<sup>2</sup>, P.Triscos<sup>6</sup>, G.Tristram<sup>6</sup>, G.Villet<sup>4</sup>, A.Volte<sup>6</sup>,  
 M.Wayne<sup>7</sup>, D.M.Websdale<sup>5</sup>, G.Wormser<sup>7</sup>, Y.Zolnierowski<sup>2</sup>

(The NA14/2 Collaboration)

**Abstract**

Kinematic correlations between the charmed  $D$  and  $\bar{D}$  mesons produced by a photon beam of mean energy 100 GeV/c have been measured by the NA14/2 experiment at CERN using a sample of almost background-free fully reconstructed  $D\bar{D}$  events. The observed  $D$  and  $D\bar{D}$  distributions are compared to the predictions of production models using different parameters for the charm fragmentation function and for the intrinsic transverse momentum of the partons.

---

<sup>1</sup>Universidad Autónoma de Barcelona, Bellaterra, Spain

<sup>2</sup>CERN, Geneva, Switzerland

<sup>3</sup>CRN, IN2P3-CNRS, and Univ. L.Pasteur, Strasbourg, France

<sup>4</sup>DPhPE, CEN-Saclay, France

<sup>5</sup>Blackett Lab., Imperial College, London, UK

<sup>6</sup>Collège de France, Paris, France

<sup>7</sup>LAL, IN2P3-CNRS, and Univ. Paris-Sud, Orsay, France

<sup>8</sup>National Technical University, Athens, Greece

<sup>9</sup>University of Warsaw, Warsaw, Poland

<sup>10</sup>University of Southampton, Southampton, UK

<sup>a</sup>Univ. J.Fourier and ISN, Grenoble, France

<sup>b</sup>Univ. Politecnica de Catalunya, ETSEIB-DEN, Barcelona, Spain

<sup>c</sup>Univ. di Roma-2, Tor Vergata, Roma, Italy

<sup>d</sup>IFIC, Centro Mixto Univ. de Valencia-CSIC, Valencia, Spain

<sup>e</sup>On leave from Fac. de Ciencias Fisicas, Univ. Complutense, Madrid, Spain

To be submitted to Phys. Lett. B



## 1. Introduction

First-order QCD predictions together with the standard Lund fragmentation model are able to reproduce most of the kinematic properties of the charmed mesons. However, this simple scheme leads only to a back-to-back production of the  $c$  and the  $\bar{c}$  in the transverse plane; therefore the correlations in the  $D\bar{D}$  system are expected to be sensitive to higher-order QCD corrections.

Little has been reported on the study of events where both charmed particles have been fully reconstructed. Up to now, one photoproduction experiment [1] has studied them, with only topological identification of the second charmed particle. Correlations in the  $D\bar{D}$  system have also been studied by hadroproduction experiments [2],[3],[4] but the photoproduction mechanism is simpler than hadroproduction where more diagrams are involved at lowest order.

## 2. Apparatus

The experiment used the NA14 spectrometer [5] which has a wide angular acceptance for neutral and charged particles, up to 300 mrad in the laboratory frame, corresponding to 5–130 degrees in the photon-nucleon centre-of-mass frame.

The photon beam interacts in a silicon active target [6]; downstream of the target a microstrip system [7] consisting of ten silicon planes with 50  $\mu\text{m}$  pitch permits an accurate determination of both decay vertices and of the production vertex [8]. Two magnets and three sets of multiwire proportional chambers allow accurate momentum measurements.

One air-filled threshold Cherenkov counter is used for particle identification, with momentum thresholds at 5.7 GeV/ $c$  for the  $\pi$ , 20.3 GeV/ $c$  for the  $K$  and 38.5 GeV/ $c$  for the proton.

## 3. Charmed Particle Selection

During the two data-taking periods in 1985-1986, 17 million triggers were recorded. The raw data were filtered to increase the charm content without looking for any specific particle. This “microstrip” filter [8] uses the vertex topology, rather than particle identification, to extract a charm-enriched sample.

The tracks seen in the chambers are then matched with the corresponding hits in the microstrips. The longitudinal position of the interaction point is obtained using the information from the active target and matched tracks are extrapolated to this position to define the production vertex coordinates in the transverse plane. The events for which all tracks are compatible with a single vertex are rejected.

For subsequent analysis, two samples were selected. The first, having one reconstructed charmed particle, was used for the inclusive study of  $D$  mesons. The second, having at least two reconstructed charmed particles, was used for the study of the  $D\bar{D}$  system.

### 3.1 The “Single Charm” Sample (at least one $D$ or $\bar{D}$ reconstructed)

The selection procedure outlined below is the same as that used in our measurement of charm lifetimes [8].

The identification of kaons is important for most of the charm decays studied in NA14. If one uses the “unambiguous” Cherenkov identification, kaons can be distinguished from pions only in a restricted momentum region (6.3–20.5 GeV/ $c$ ). This limits the number of kaons available for analysis. To improve the  $K$  acceptance an “extended kaon” region was defined which includes the  $\pi/K$  ambiguous region above 20 GeV/ $c$ .

One, two or three pions are combined with the selected kaon. These tracks are used to find the decay vertex and a  $P(\chi^2) > 0.001$  criterion is used to reject bad decay vertices. The trajectory of the candidate charmed particle is then reconstructed and is used, together with the remaining tracks in the event, to reconstruct the production vertex. Depending on the  $\chi^2$  probability of the vertex fit, the least well-associated track (which cannot be the charm track) is rejected and the process is iterated until  $P(\chi^2) > 0.001$  or only the charmed track is left.

A large sample of  $D$  mesons is extracted by imposing a cut on the separation between the interaction and the decay vertices, weighted by the corresponding error:

$$N_\sigma = \frac{\Delta x}{\sigma_{\Delta x}}.$$

In order to optimize the signal to background ratio, we use different  $N_\sigma$  cuts for the three decay channels under investigation:  $N_\sigma > 2$  for  $D^0 \rightarrow K^-\pi^+$ ,  $N_\sigma > 4$  for  $D^+ \rightarrow K^-\pi^+\pi^+$  and  $N_\sigma > 6$  for  $D^0 \rightarrow K^-\pi^+\pi^+\pi^-$ .

The presence of a  $D^*$  ( $D^{*+} \rightarrow D^0\pi^+$ ) is easily tagged by computing the mass difference  $\Delta M = M(D^*) - M(D)$  and this allows a less severe cut. In this case we use:  $N_\sigma > 0.5$  for  $D^0 \rightarrow K^-\pi^+$  and  $N_\sigma > 4$  for  $D^0 \rightarrow K^-\pi^+\pi^+\pi^-$ .

This gives us a sample of  $1134 \pm 43 D$  (or  $\bar{D}$ ) mesons, with a signal to background ratio of  $1.7 \pm 0.1$ .

For this “single charm” sample, the signal events are taken from the mass interval 1.835 – 1.875 GeV/ $c^2$ , and background subtractions are made using events outside this mass interval.

### 3.2 The “Double Charm” Sample (both $D$ and $\bar{D}$ reconstructed)

To obtain a background-free sample, the “unambiguous”  $K$  identification is used. One, two or three pions are combined with the selected kaon. The invariant mass of the combination is first required to be in the mass range 1.7 – 2.0 GeV/ $c^2$ .

We then search for secondary vertices, one for each charm candidate. If the two vertices are found, the trajectory of each charmed particle is reconstructed. The production vertex fit is performed using the two charm tracks together with the remaining charged tracks. A  $P(\chi^2) > 0.002$  cut is imposed. If the fit fails, the track with the largest contribution to the  $\chi^2$  is dropped (the two charm tracks cannot be dropped). This procedure is repeated until the cut is passed. We use a tighter  $P(\chi^2)$  criterion than for the single charm sample

because now the two reconstructed charm tracks are present in the production vertex computation.

An example of a double charm event is shown in fig. 1. The high ionization at the interaction in the active target is clearly seen as is the step increase at the decay.

To avoid double counting only one topological combination is selected per event. The probability of  $\chi^2$  of the three vertices is used to define a weight for each combination in a given event and the combination with the largest weight is chosen.

For the “double charm” sample, events are accepted where both charm candidates have a mass in the range  $1.82 - 1.88 \text{ GeV}/c^2$  and no background is subtracted.

This produced a total of 22 fully reconstructed  $D\bar{D}$  events, with a negligible background (fig. 2). The numbers of events in each channel are:

$5K\pi K\pi$ ,  $4K\pi K\pi\pi$ ,  $5K\pi K\pi\pi\pi$ ,  $1K\pi\pi K\pi\pi$ ,  $2K\pi\pi K\pi\pi\pi$ ,  $5K\pi\pi\pi K\pi\pi\pi$

We searched also for events containing more than two charmed particles. In this case the tag is the detection of two particles with the same charm quantum number ( $DD$  or  $\bar{D}\bar{D}$  as opposed to  $D\bar{D}$ ). No charm candidate is found when the other is selected in the  $1.82 - 1.88 \text{ GeV}/c^2$  mass region.

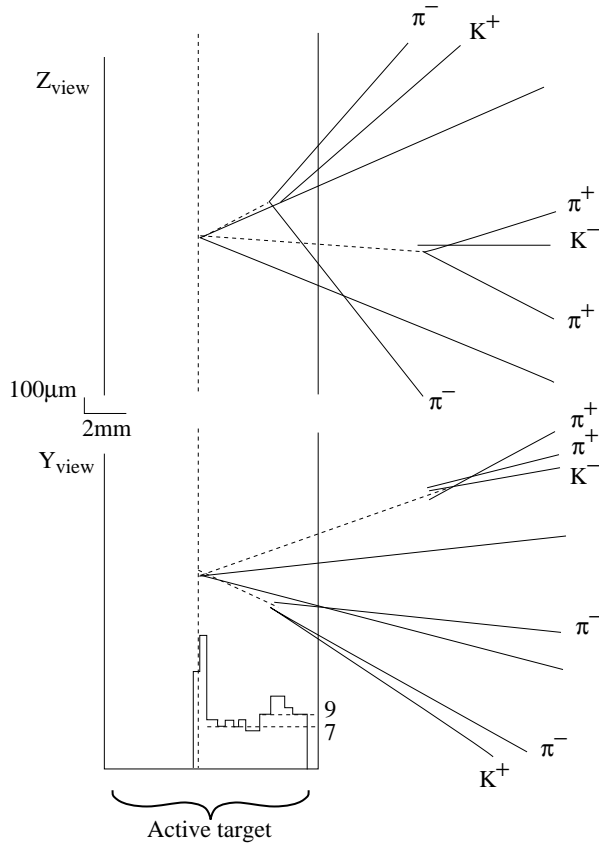


Figure 1: A fully reconstructed  $D^+D^-$  event with  $D^- \rightarrow K^+\pi^-\pi^-$  and  $D^+ \rightarrow K^-\pi^+\pi^+$ . A step in charged multiplicity corresponding to the decay of the first charmed particle is seen in the active target.

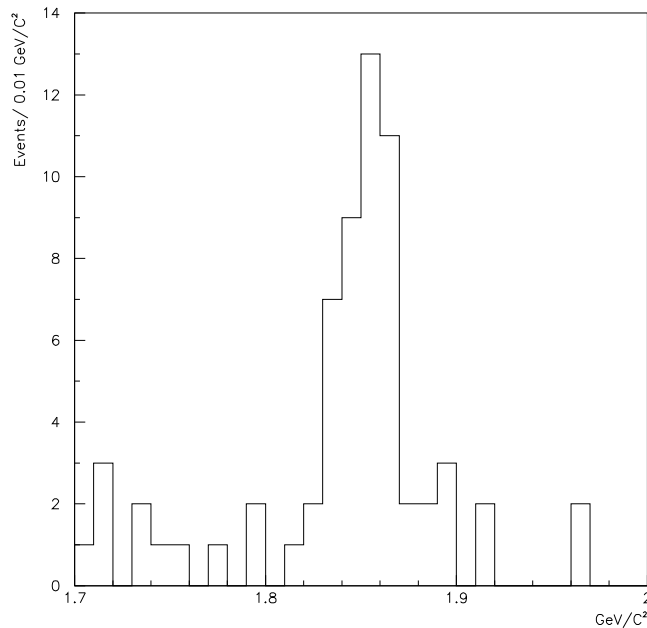


Figure 2:  $K\pi$ ,  $K\pi\pi$  or  $K\pi\pi\pi$  mass distribution when the reconstructed mass of the other charmed particle is between  $1.82$  and  $1.88 \text{ GeV}/c^2$

#### 4. Production Model

To model charm production, the first-order QCD calculation (photon-gluon fusion) is used and the hadronization is described using the dual parton model [9] where a single topological graph (fig. 3) is expected to dominate.

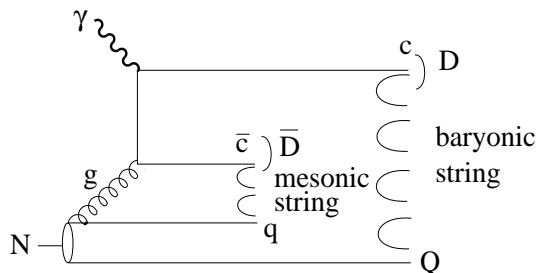


Figure 3: Photon-gluon fusion in the dual parton model.

A gluon structure-function  $xG(x) = 3(1-x)^5$  is taken. No  $Q^2$  evolution is introduced and a value  $Q^2 = 4m_c^2$  is selected. The mass of the charmed quark is taken as  $m_c = 1.5 \text{ GeV}/c^2$ . This value is compatible with what we determined in another publication [10].

Two strings are formed. A mesonic string stretches between the charmed antiquark and a quark ( $q$ ) from the target nucleon. A baryonic string stretches between the charmed quark ( $c$ ) and the remaining diquark ( $Q$ ) of the nucleon.

A fragmentation function

$$zD(z) = (1-z) \exp(-0.7m_T^2/z)$$

is used to describe the fraction of the energy of the original string carried by the final charmed particle. The Lund model is used to hadronize the mesonic and the baryonic strings independently.

The Monte Carlo samples have been generated using this standard “soft” fragmentation function; in order to evaluate the sensitivity of the distributions to the components of the model, a “hard” fragmentation function was also tested:

$$zD(z) = \frac{1}{\sqrt{1-z}} \exp(-0.7m_T^2/z).$$

An intrinsic  $p_T$  component is given to the quarks inside the nucleon with a mean value  $\langle p_T^2 \rangle = 0.1 \text{ GeV}^2/c^2$ . In order to evaluate the sensitivity of the distributions to this parameter, values of  $\langle p_T^2 \rangle$  up to  $1 \text{ GeV}^2/c^2$  were tested.

Both Monte Carlo samples, incorporating acceptance effects for “single” or “double” charm, are analysed by the same set of programs as is used for the real data. The resulting distributions are compared with the raw experimental data.

## 5. Charm Analysis

Two analyses have been carried out. First, the inclusive study of charmed particles has been developed; the main aims were to check the effect of changing the fragmentation function and the intrinsic  $p_T$  of the quarks in the high statistics “single charm” sample and to verify that the results for the “double charm” sample were compatible. The second analysis studied the  $D\bar{D}$  system in the fully reconstructed “double charm” sample.

### 5.1 Inclusive $D$ Analysis

We study the sensitivity of the distributions of  $p_T$  (fig. 4a) and of  $p_L$  (fig. 4b) to the fragmentation function and to the intrinsic  $p_T$  of the quarks. Our results on  $x_F$  and  $p_T^2$  are detailed in another paper [10].

We observe a good fit to the data and a small dependence on Monte Carlo parameters. The soft fragmentation function seems to be preferred by the longitudinal momentum distributions ( $p_L$ ). The transverse momentum distribution ( $p_T$ ) is not very sensitive to a change of the fragmentation function. None of the quantities studied seem to be sensitive to the choice of the intrinsic  $p_T$  of the quarks, although a slight effect is noticeable in the transverse distribution.

The same inclusive analysis on the “double charm” sample gives comparable results (figs. 4c and 4d) despite different acceptances, but one can notice the reduction in the mean value of  $p_L$  when compared with the “single charm” sample. This is expected because in this sample the second charmed particle has also been found. This produces a reduction in the acceptance for large  $p_L$ , since if one of the particles is produced very forward (fast) the other will tend to be produced backward (slow) and therefore will be more difficult to detect.

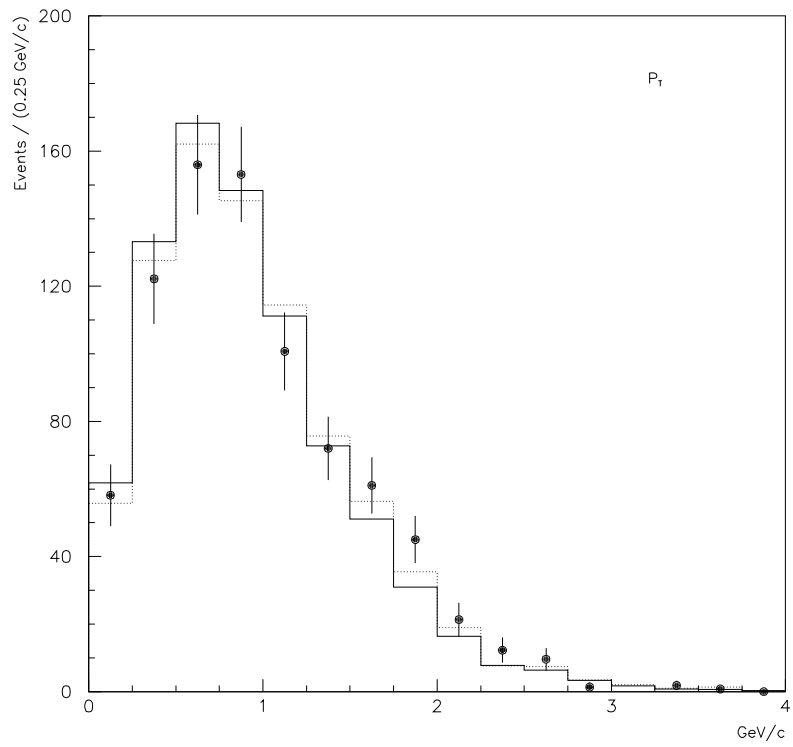


Figure 4a

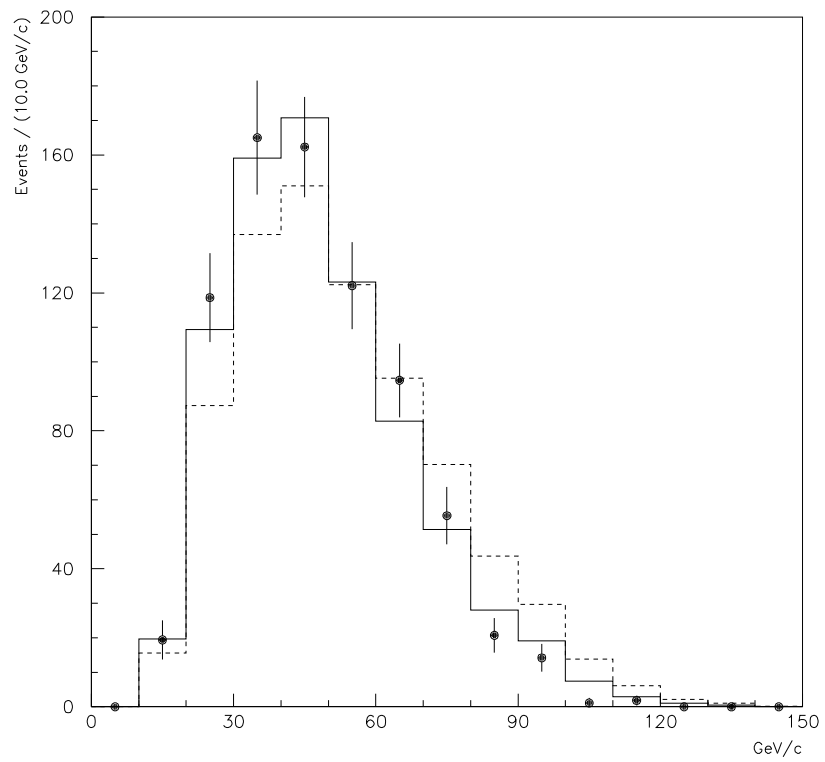
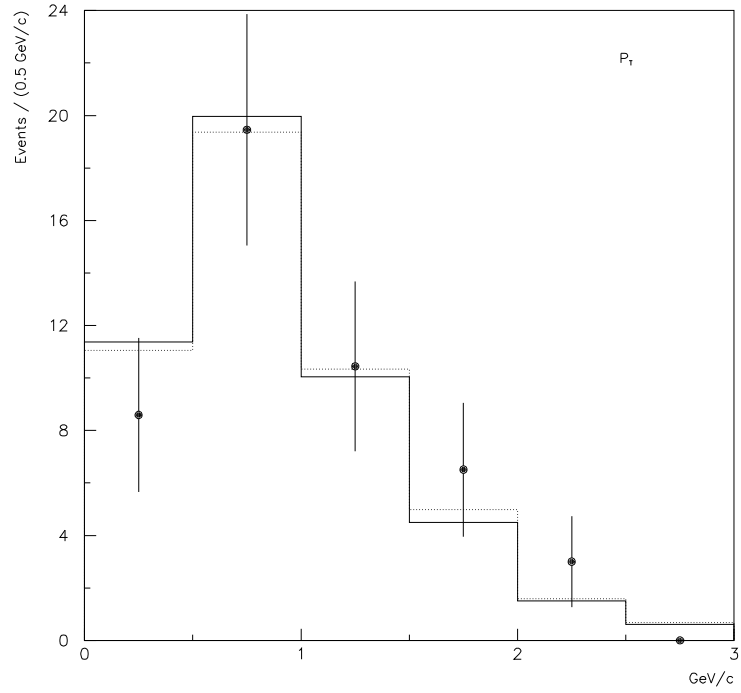
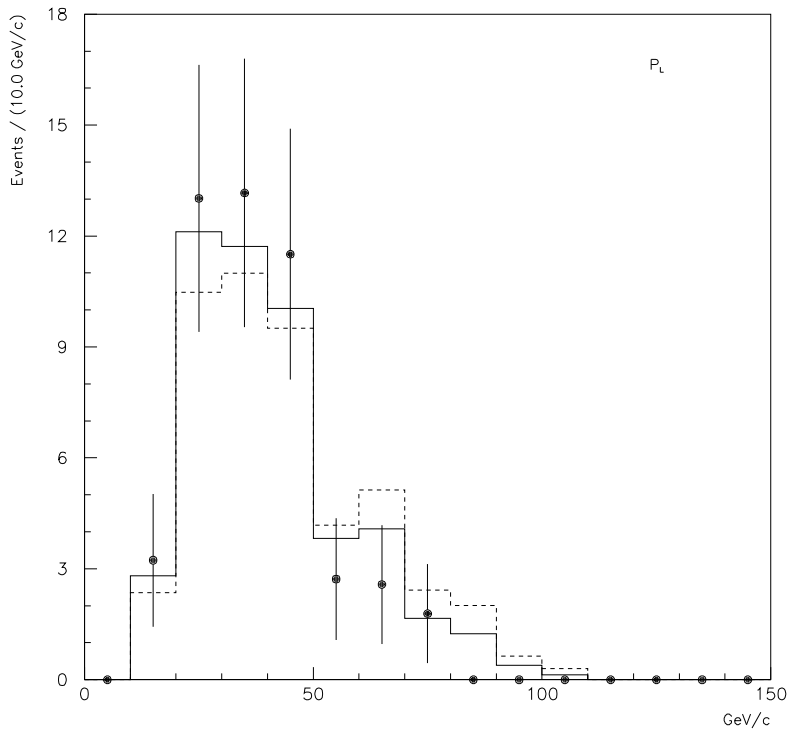


Figure 4b





(c)



(d)

Figure 4: Inclusive analysis: (a)  $p_T$  and (b)  $p_L$  of the  $D$  or of the  $\bar{D}$  (“Single charm” sample) (c)  $p_T$  and (d)  $p_L$  of the  $D$  or of the  $\bar{D}$  (“Double charm” sample).

Full line:  $0.1 \text{ GeV}^2/c^2$  of intrinsic  $p_T^2$  with soft fragmentation function.

Dotted line: (a, c)  $1.0 \text{ GeV}^2/c^2$  of intrinsic  $p_T^2$ .

Dashed line: (b, d) hard fragmentation function.

## 5.2 $D\bar{D}$ System Analysis

The agreement between the Monte Carlo simulation and the real data distributions is not so good in the study of the  $D\bar{D}$  system as it is in the inclusive analysis. The distributions of  $p_T(D\bar{D})$  (fig. 5a) and  $p_L(D\bar{D})$  (fig. 5b) show a greater sensitivity to the production parameters; the  $p_T$  distribution suggests some contribution from second-order effects.

The effect of changing the fragmentation function has a noticeable effect only on the  $p_L$  distribution; however, even with a soft fragmentation function the Monte Carlo is unable to predict the small mean value of  $p_L$  which is observed in the data (fig. 5b).

The only quantity sensitive to the intrinsic  $p_T$  of the quarks is  $p_T(D\bar{D})$ . Closer agreement between the Monte Carlo and the measured mean values is obtained using a large intrinsic  $p_T$  :  $\langle p_T^2 \rangle = 1.0 \text{ GeV}^2/c^2$  (fig 5a).

The invariant-mass distribution of the  $D\bar{D}$  system (fig. 6a) and the distribution of the difference in rapidity between the charmed particles (fig. 6b) are in agreement with expectations and show a very small sensitivity to the fragmentation function. We observe no effect due to the intrinsic  $p_T$  of the quarks.

The angle  $\phi$  (fig. 6c) between the two transverse components of the momentum of the two reconstructed charmed particles is used to study the back-to-back behaviour of the charm-anticharm system. The predictions for  $\phi$  are also compatible with the data, but a flatter distribution would yield a better agreement and suggest also some influence of second-order effects.

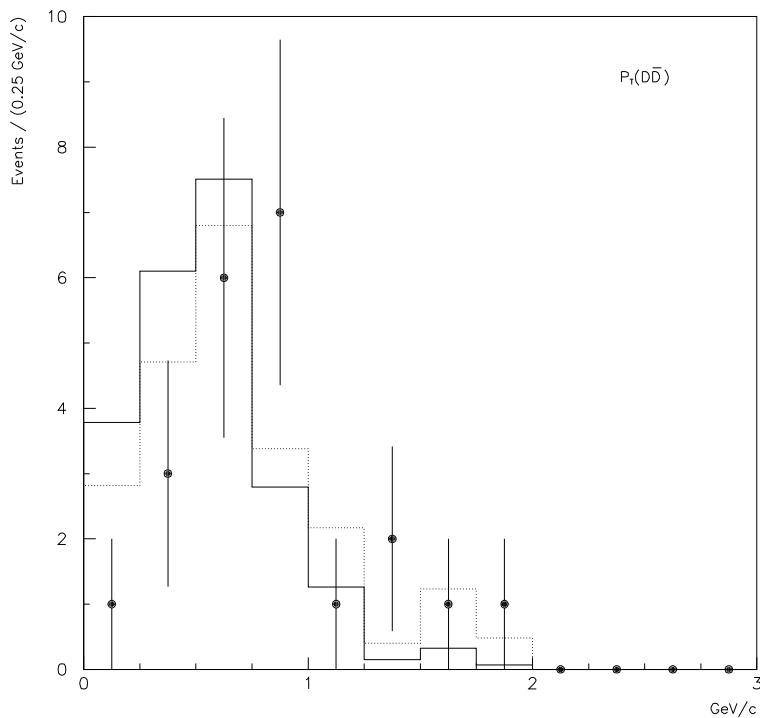
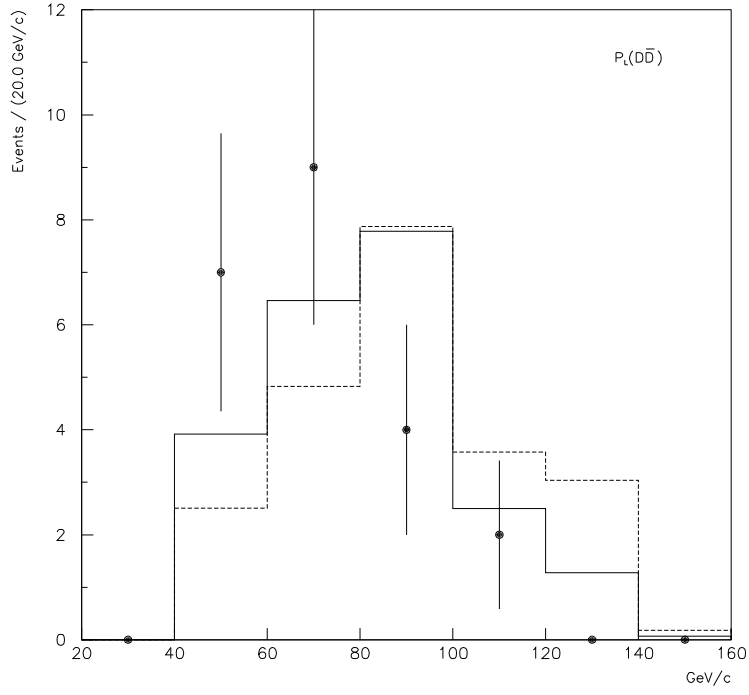


Figure 5a



(b)

Figure 5: (a)  $p_T$  and (b)  $p_L$  of the  $D\bar{D}$  system (“Double charm” sample).

Full line:  $0.1 \text{ GeV}^2/c^2$  of intrinsic  $p_T^2$  with soft fragmentation function.

Dotted line: (a)  $1.0 \text{ GeV}^2/c^2$  of intrinsic  $p_T^2$ .

Dashed line: (b) hard fragmentation function.

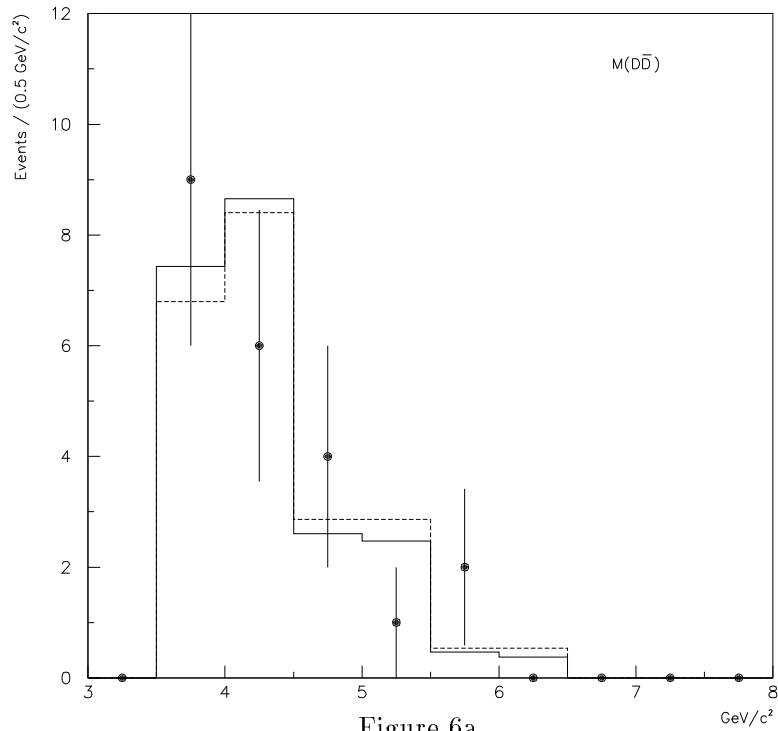
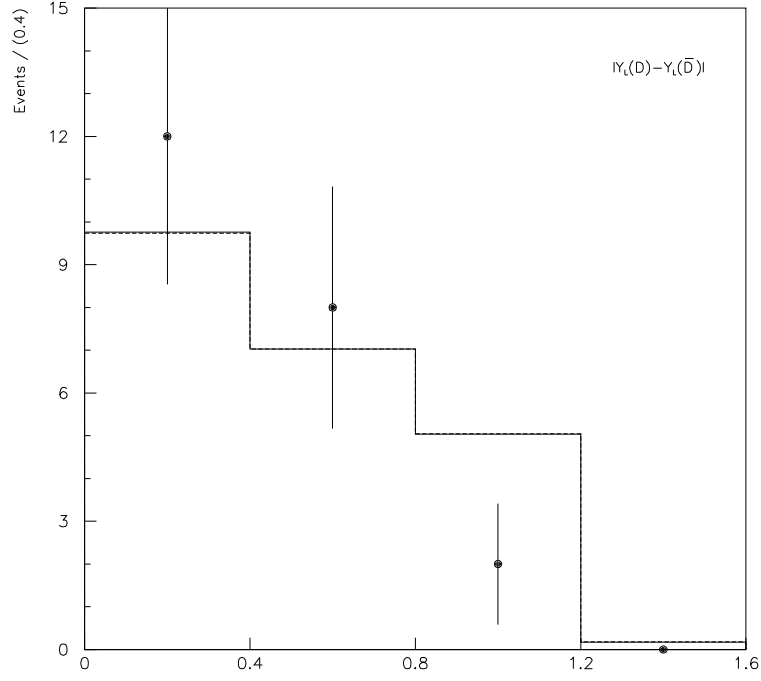
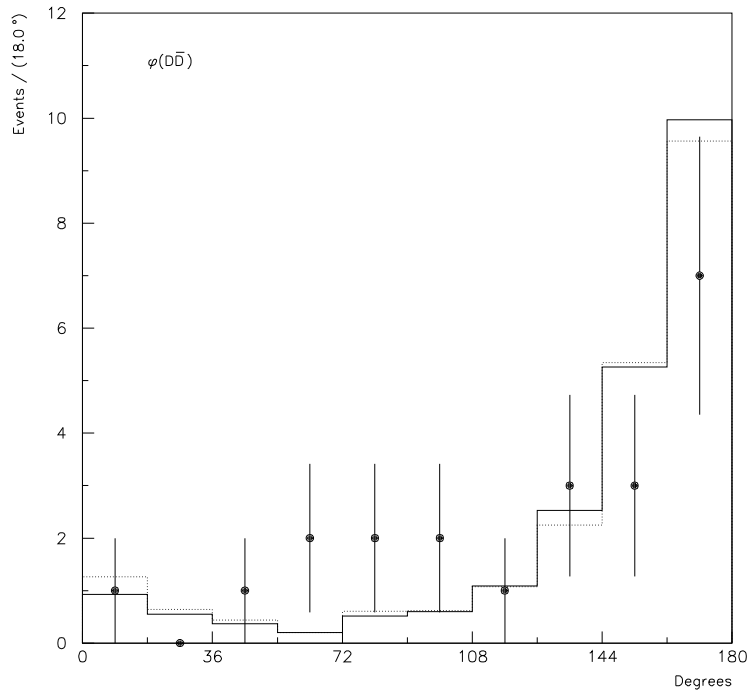


Figure 6a



(b)



(c)

Figure 6: Properties of the  $D\bar{D}$  system: (a) Mass of the  $D\bar{D}$  system (b) Difference in rapidity between the  $D$  and the  $\bar{D}$  (folded); (c) Angle  $\phi$  between the transverse momenta of the  $D$  and the  $\bar{D}$ .

Full line: (a) (b) (c)  $0.1 \text{ GeV}^2/c^2$  of intrinsic  $p_T^2$  with soft fragmentation function.

Dashed line: (a) (b) hard fragmentation function.

Dotted line: (c)  $1.0 \text{ GeV}^2/c^2$  of intrinsic  $p_T^2$ .

### 5.3 Effects of Gluon Intrinsic $p_T$

To study the influence of an intrinsic  $p_T$  component of the gluon inside the nucleon, we have introduced this as an additional degree of freedom in the Monte Carlo simulation. In doing so, we assume that the transverse momentum of the gluon is compensated by that taken by the constituent quark and diquark; these last two objects also have a relative  $p_T$ , with  $\langle p_T^2 \rangle = 0.1 \text{ GeV}^2/c^2$ , characteristic of soft hadronic interactions.

We try to analyse the effect due to the transverse gluon momentum because it may affect more directly the properties of the  $D\bar{D}$  system.

To satisfy energy and momentum conservation, partons with off-shell masses are used. When the nucleon target splits into two systems (the gluon and the quark-diquark cluster), its mass is related to the transverse masses of the two systems in the following way:

$$m_N^2 = \frac{m_{TqQ}^2}{(1-x_G)} + \frac{m_{TG}^2}{x_G} \quad \text{where} \quad x_G = \frac{(E_G + p_{LG})}{(E_N + p_{LN})}.$$

Because of the  $x$ -dependence of the gluon structure-function,  $x_G$  is usually close to its threshold value, so to prevent unphysical behaviour at small  $x_G$  we assume that  $m_{TG} = 0$ , implying that  $m_G^2 = -p_{TG}^2$ .

The result of the simulation for individual charmed particles is only a small effect : the intrinsic  $p_T$  of the gluon has to be shared between the two charmed quarks; the target spectator quark or diquark are emitted with a total transverse momentum opposite to the gluon intrinsic  $p_T$ ; therefore the transverse momentum of the string along which a  $D$  particle is generated is much smaller than the original  $p_T$  of the gluon. Hence the effect of the intrinsic  $p_T$  of the gluon on the  $p_T$  of individual charmed particles is largely diluted.

The simulation shows that a better agreement for the  $p_T(D\bar{D})$  distribution could be obtained by increasing the intrinsic  $p_T^2$  of the gluon up to the improbable value of  $1 \text{ GeV}^2/c^2$ , but this does not produce a comparable improvement in the agreement with the  $\phi$  distribution. Because of its low sensitivity to the intrinsic  $p_T$ , the  $\phi$  distribution could be a good indicator of the effect of higher-order QCD corrections where the  $p_T$  of the gluon is not necessarily compensated by that of the  $qQ$  cluster.

## 6. Conclusions

An essentially background-free sample of 22 fully reconstructed  $D\bar{D}$  events was extracted from 17 million photon interaction triggers. This represents the largest sample of fully reconstructed double charm events published to date in a photoproduction experiment.

The sensitivities of the inclusive  $D$  distributions and of the  $D\bar{D}$  system distributions to the parameters of the charm fragmentation function and of the intrinsic transverse momentum of the partons have been studied.

The abundance of ‘‘single charm’’ events has made possible the fine-tuning of the hadronization models in inclusive production.

The  $p_T$  and  $p_L$  distributions of each  $D$  and the mass of the  $D\bar{D}$  system are well fitted by the model but are not very sensitive to the parameters. The  $p_T$ ,  $p_L$  and  $\phi$  distributions of the  $D\bar{D}$  system seem to be more sensitive to these parameters; in particular, the  $p_T$  and  $\phi$  distributions would suggest some contribution from second-order effects.

## REFERENCES

- [1] M.I.Adamovich et al., Phys. Lett. 140B (1984) 119 and 123.
- [2] M. Aguilar-Benitez et al., Phys. Lett. **164B** (1985) 404.
- [3] M. Aguilar-Benitez et al., Z. Phys. **C 40** (1988) 321
- [4] Fermilab E653 Collaboration, Washington APS Meeting, April, 1990 and XXVth Rencontres de Moriond, Les Arcs, 1990.
- [5] P. Astbury et al., Phys. Lett. **152B** (1985) 419.
- [6] R. Barate et al., Nucl. Instr. Meth. **A235** (1985) 235.
- [7] G. Barber et al., Nucl. Instr. Meth. **A253** (1987) 530.
- [8] M.P. Alvarez et al., Z. Phys. **C 47** (1990) 539.
- [9] A. Capella and J. Tran Thanh Van, Phys. Lett. **93B** (1980) 146;  
P.Roudeau: Nucl. Phys. B (Proc. Suppl.) **1B** (1988) 33.
- [10] M.P. Alvarez et al., submitted to Z. Phys. C